Reduction of the Iron−Sulfur Clusters in Mitochondrial NADH:Ubiquinone Oxidoreductase (Complex I) by Eu^{II}-DTPA, a Very Low Potential Reductant[†]

Torsten Reda, Chérise D. Barker, and Judy Hirst*

Medical Research Council Dunn Human Nutrition Unit, Wellcome Trust/MRC Building, Hills Road, Cambridge, CB2 0XY, U.K.

Received March 14, 2008; Revised Manuscript Received June 27, 2008

ABSTRACT: NADH:ubiquinone oxidoreductase (complex I) is the first enzyme of the mitochondrial electron transport chain. It contains a flavin mononucleotide to oxidize NADH, and eight iron-sulfur clusters. Seven of them transfer electrons between the flavin and the quinone-binding site, and one is on the opposite side of the flavin. Although most information about their properties is from EPR, the spectra from only five clusters have been observed, and it is difficult to match them to the structurally defined clusters. Here, we analyze complex I from bovine mitochondria reacted with a very low potential reductant, to impose a potential approaching −1 V. We compare the spectra with those from higher potentials and from the 24 kDa subunit and flavoprotein subcomplex, and model the spectra by starting from those with fewer components and building the complexity gradually. Spectrum N1a, from the 24 kDa subunit [2Fe-2S] cluster, is not observed in bovine complex I at any potential. Spectrum N1b, from the 75 kDa subunit [2Fe-2S] cluster, exhibits a lower potential than the N3, N4 and N5 spectra of three [4Fe-4S] clusters. In the lowest potential spectra an N5-type spectrum is observed at unusually high temperature (indicating a significant change to the cluster, or that two clusters have very similar *g* values), the relaxation rate of N1b increases (indicating that a nearby cluster has become reduced) and a new feature with an apparent *g* value of 2.16 suggests an interaction between two reduced clusters. The consequences of these observations for electron transfer in complex I are discussed.

Complex I (NADH:ubiquinone oxidoreductase) is the first enzyme of the electron transport chain in many aerobically respiring organisms (*1–3*). In bovine mitochondria it comprises forty-five different subunits (*4*), and it is arranged in two major domains, a hydrophobic domain in the inner mitochondrial membrane, and a hydrophilic domain which extends into the mitochondrial matrix. NADH is oxidized to NAD^+ by a flavin mononucleotide (FMN[1]) cofactor located in the hydrophilic domain, and ubiquinone is reduced to ubiquinol in the hydrophobic domain. The two substrate binding sites are separated from one another by more than 70 Å (*5*), so the transfer of electrons between them is mediated by a "chain" of iron−sulfur (FeS) clusters. The electron transfer process must conserve the energy from the redox reaction as the proton motive force across the mitochondrial inner membrane. The structure of the hydrophilic domain of complex I from *Thermus thermophilus* provides the best available model for the structure of the subunits which coordinate the FeS clusters and the FMN in mitochondrial complex I,[2] and for the relative positions of the cofactors (see Figure 1) (*5*). Current knowledge of the properties of the FeS clusters in complex I has been derived predominantly from electron paramagnetic resonance (EPR), and extensive studies, particularly of the bovine enzyme, have been undertaken (see for example refs *6–8*). The enzyme's complexity renders the interpretation of spectroscopic data difficult, so the elucidation of its structure provides new opportunities for the development of an integrated and self-consistent picture.

Complex I from bovine mitochondria contains eight FeS clusters (*5, 8–10*) (see Figure 1). Seven of them form the chain of clusters which extend between the FMN and the ubiquinone binding site, whereas the eighth cluster is located on the opposite side of the FMN (*5*). Its role is not defined clearly at present (*1, 11*). Only five reduced FeS clusters have been observed in the EPR spectra of bovine complex I (*8*), and these have the EPR spectra referred to as N1b, N2, N3, N4 and N5. N1b is from the [2Fe-2S] cluster in the 75 kDa subunit (cluster 2Fe[75]). The distal [2Fe-2S] cluster in the 24 kDa subunit (cluster 2Fe[24]) displays the spectrum named N1a in reduced *Escherichia coli* complex I (*12*), but has not been observed in reduced bovine complex I (*13*). The initial and final clusters in the chain (4Fe[51] and 4Fe[PS]) display the N3 and N2 spectra, respectively (*8, 14*). Assignment of the N4 and N5 spectra to specific clusters is

[†] This research was funded by The Medical Research Council and the European Union Mitocombat program.

* Address correspondence to this author at Medical Research Council Dunn Human Nutrition Unit, Wellcome Trust/MRC Building, Hills Road, Cambridge, CB2 0XY, U.K. Tel: +44 1223 252810. Fax: +44 1223 252815. E-mail: jh@mrc-dunn.cam.ac.uk.

[1] Abbreviations: DTPA, diethylenetriamine-*N*,*N*,*N*′,*N*″,*N*″-pentaacetate; EPR, electron paramagnetic resonance; FeS, iron−sulfur; FMN, flavin mononucleotide; FP, flavoprotein subcomplex of complex I.

[2] In bovine complex I the iron−sulfur clusters are ligated by five subunits, the 75 kDa, 51 kDa, 24 kDa, PSST and TYKY subunits (PSST and TYKY are the first four amino acids in the mature proteins). They are homologous, respectively, to the NuoG, NuoF, NuoE, NuoB and NuoI subunits in *Escherichia coli*, the Nqo3, Nqo1, Nqo2, Nqo9 and Nqo6 subunits in *Thermus thermophilus*, the NUAM, NUBM, NUHN, NUIM and NUKM subunits in *Yarrowia lipolytica*, and to the NDUFS1, NDUFV1, NDUFV2, NDUFS8 and NDUFS7 subunits in *Homo sapiens*.

10.1021/bi800437g CCC: $40.75
Published on Web 07/24/2008

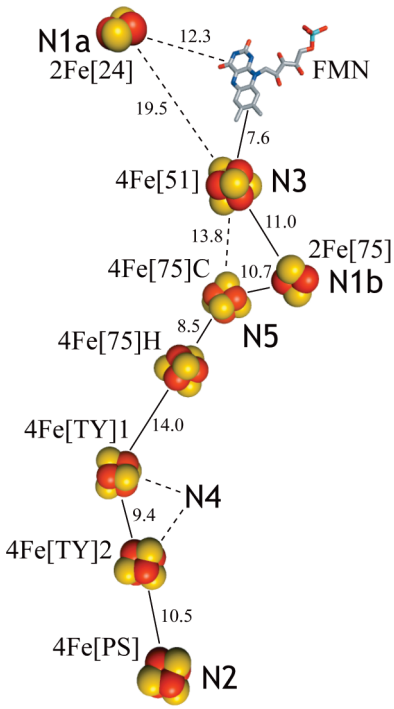

FIGURE 1: Cofactor distribution and schematic representation of the electron pathway through complex I. The positions and edge-to-edge distances of the FMN, the two [2Fe-2S], and six [4Fe-4S] clusters are shown, according to structural information from the hydrophilic domain of *T. thermophilus* complex I (*5*). The clusters are named for their nuclearity (2Fe or 4Fe), their subunit (75, 51 24 kDa, TYKY or PSST, abbreviated here to TY or PS) and, when necessary, as C (all cysteine ligated) or H (three cysteine ligands, one histidine ligand). Their EPR spectra are named N1a, N1b (2Fe clusters), N2, N3, N4 and N5 (4Fe clusters), and the assignment of spectra to clusters is taken from ref *10*.

problematic. Ohnishi and co-workers assigned both spectra to the 75 kDa subunit (*8*), but we have proposed recently that N4 should be assigned to the TYKY subunit instead (*10*). In addition to the 2Fe[24] cluster, two 4Fe clusters remain undetected in the EPR spectra of reduced bovine complex I, and so nothing is currently known about their properties. The nomenclature used here for the FeS clusters in complex I is defined in Figure 1. The clusters are named for their nuclearity (2Fe or 4Fe), their subunit (75, 51 or 24 kDa, TYKY or PSST) and, when necessary, as C (all cysteine ligated) or H (three cysteine ligands, one histidine ligand). Their EPR spectra are named N1a, N1b (2Fe clusters), N2, N3, N4 and N5 (4Fe clusters).

Here, we use the low potential reductant Eu^{II}-DTPA (Eu^{II}-diethylenetriamine-*N*,*N*′,*N*′,*N*″,*N*″-pentaacetate) (*15*) to impose a strongly reducing potential (close to −1 V) on bovine complex I. We compare the spectra of complex I samples at higher potentials with those at very low potential, and model the spectra by starting from those with fewer components and progressing toward the most complex spectra gradually, to arrive at the most internally consistent description. Thus, we aim to investigate the three clusters which have not so far been observed in reduced mitochondrial complex I by EPR, to obtain further information about the properties of those clusters which have already been observed, and to identify possible interactions between the reduced clusters. Definition of the properties of the individual clusters, and of the cluster ensemble, is an important part of defining the

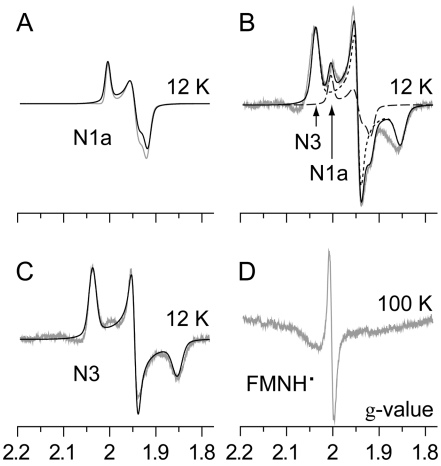

FIGURE 2: EPR spectra of the 24 kDa subunit of bovine complex I and the flavoprotein subcomplex (FP). (A) The purified, overexpressed 24 kDa subunit reduced by 2 mM dithionite at pH 7.8 recorded at 12 K (gray) and the simulated spectrum (black) (B) FP reduced by 2 mM dithionite at pH 7.8 recorded at 12 K (gray) with the simulated spectrum (black), constructed from N1a (parameters from A, dashed line) and N3 (parameters from C, dotted line). (C) FP reduced by 2 mM NADH at pH 7.8 recorded at 12 K (gray) and simulated (black). (D) Radical spectrum from FP reduced with NADH at 100 K, probably from the flavin semiquinone. The spectra in A and C have been scaled to match those in B. C and D are from the same sample; they were normalized for temperature using the Curie Law, and then the intensity of D was scaled by 0.2. See Table 1 for simulation parameters.

mechanisms of energy transduction and reactive oxygen species generation by complex I.

MATERIALS AND METHODS

Sample Preparation. The 24 kDa subunit from bovine complex I, the flavoprotein subcomplex (FP) of bovine complex I, and complex I from bovine heart mitochondria were prepared as described previously (*16*–*18*); the protein composition of the complex I preparation has been characterized and described in detail (*9*). Each sample was dialyzed at 4 °C inside an anaerobic chamber (Belle Technology, O_2 < 5 ppm) to remove residual O_2 before it was reduced, and all samples were both prepared and frozen (within two to five minutes) inside the anaerobic chamber. The redox mediator cocktail (inset to Figure 3) comprised 25 μM phenazine, phenosafranin, neutral red (Sigma), and 50 μM methyl viologen (Fluka). The redox potential was set using sodium dithionite (Sigma) and monitored using a platinum electrode and an Ag/AgCl, saturated KCl reference electrode. NADH (Sigma) was repurified before use (*19*) to remove NAD^+. Complex I was reduced to very low potential using Eu^{II}-DTPA (*15*). 2 mM Eu^{2+} was generated by the bulk electrolysis of Eu_2O_3 [10 μL of 50 mM Eu_2O_3 (Aldrich) in 0.5 M HCl was added to 0.49 mL of 50 mM Tris-HCl pH 7 and 100 mM NaCl] in a graphite "pot" electrode. A small magnetic stirrer was used to agitate the solution, and an applied potential of −0.6 V reduced the Eu^{3+} to Eu^{2+} completely within 15 min (total charge passed > 0.95[Eu^{III}]). Eu^{II}-DTPA was generated in situ by the addition of 1.3 mM DTPA (Fluka, from a 50 mM stock solution in 0.2 M NaOH) to a solution containing 0.65 mM Eu^{2+} and ~20 mg mL^{-1} of complex I, resulting in 22 Eu^{II}-DTPA molecules for every

complex I (a 2.2-fold excess of reducing equivalents, assuming complex I requires ten electrons to become fully reduced).

EPR Spectroscopy. EPR measurements were conducted using an X-band Bruker EMX spectrometer (Bruker BioSpin GmbH, Germany) with an ER4119HS high-sensitivity cavity. The sample temperatures were controlled using an ESR 900 helium flow cryostat (Oxford Instruments, U.K.), and measured with a calibrated Cernox resistor (Lake Shore Cryotronics Inc., OH). Unless stated otherwise the modulation amplitude was 5 G at 100 kHz and the microwave power was 0.5 mW. The magnetic field was calibrated using strong and weak pitch standards. The spectrometer configuration does not include a microwave frequency counter (microwave frequency ± 5 MHz).

Spectra Normalization and Simulation. All samples were prepared at approximately 20 mg mL^{-1} protein. To account for small variations in protein concentration all complex I spectra were normalized to the intensity of an internal reference, the simulated $N2_z$ signal at 12 K. Simulations were performed using WINEPR SimFonia Version 1.25 (Bruker BioSpin GmbH, Germany). The simulated spectra are defined by their g values (x, y, z), line widths (L, the half-width at half-height) and line shapes (R, the relative contributions from the Lorentzian ($R = 1$) and Gaussian ($R = 0$) line shapes).

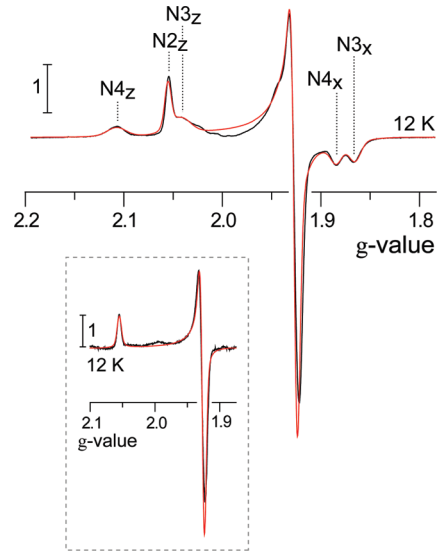

FIGURE 3: EPR spectra of complex I poised at −0.3 V using NADH and NAD^+, and poised potentiometrically at −0.1 V. Main figure: Complex I was reduced using a total of 2 mM NAD^+ + NADH at a ratio of 29.94 to 1, to set the potential to −0.3 V (pH 7.8); the NADH oxidized by the protein was taken into account. The spectrum recorded at 12 K (black) is compared to the simulated spectrum (red), comprising N2, N3, and N4. Inset: Complex I was titrated in a mixture of redox mediators, using sodium dithionite, to −0.1 V at pH 7.8. The spectrum recorded at 12 K (black) is compared to the simulated N2 spectrum (red). The scale bars refer to the height of the modeled $N2_z$ feature. See Table 1 for parameters.

RESULTS

The 24 kDa Subunit and the FP Subcomplex (Spectra N1a and N3). The EPR spectrum of the reduced [2Fe-2S] cluster in the overexpressed 24 kDa subunit of complex I from bovine mitochondria (cluster 2Fe[24]) is shown in Figure 2A (*16*). The typical rhombic spectrum, N1a, has been modeled using the parameters in Table 1. The spectrum from the isolated subunit is clearly visible over an extended temperature range, from 4 to 100 K (see Figure S2A, Supporting Information), and the spectrum in Figure 2A was recorded at 12 K, under the conditions used for comparison throughout this study. The g_z signal is prominent at $g \sim 2$, clearly separated from the other signals (see below).

The flavoprotein (FP) subcomplex of bovine complex I contains the FMN at the active site for NADH oxidation, cluster 2Fe[24], and the [4Fe-4S] cluster in the 51 kDa subunit (cluster 4Fe[51]) (*17, 20*). When FP is reduced with sodium dithionite N1a and N3 are observed, from the reduced 2Fe[24] and 4Fe[51] clusters, respectively (see Figure 2B). N1a dominates at higher temperature (see Figure S2B), and the spectrum at 12 K can be modeled accurately by combining N1a and N3 (see Table 1 for parameters). Only N3 is visible in the spectrum of FP reduced by NADH (see Figure 2C), showing that 2Fe[24] is not reduced; voltammetric studies on the overexpressed bovine 24 kDa subunit suggested previously that its potential is below that of NADH (*16*). At high temperature (100 K, see Figure 2D) an additional isotropic spectrum is observed in the NADH-reduced FP sample. It corresponds well to the spectrum of the semiflavoquinone radical in complex I ($g = 2.002$, $L =$ 0.75 mT at 100 K (Table 1) vs $g = 2.005$ and $L = 0.85$ mT at 169 K (with L defined as half-width at half-height) (*14*)). The reduction of the 2Fe[24] cluster and formation of the semiflavoquinone in FP are discussed below.

The [4Fe-4S] Cluster in PSST (Spectrum N2) in Complex I. Complex I poised at a moderately reducing potential displayed, as expected (*8*), essentially only spectrum N2 (see inset to Figure 3), attributed to the [4Fe-4S] cluster in subunit PSST, cluster 4Fe[PS]. N2 is clearest at intermediate temperatures (9 to 25 K, see Figure S3A, Supporting Information), and it can be modeled accurately using an axial spectrum (see Table 1 for parameters). 4Fe[PS] has the highest reduction potential of all the EPR-visible clusters in complex I (*8*), so that we consider it fully reduced in all the lower potential samples and use the intensity of the modeled $N2_z$ signal (at $g = 2.055$, 12 K) for normalization; we use the modeled signal to avoid interference from adjacent overlapping signals.

The N1b, N3, N4 and N5 Spectra in Complex I. Figure 3 shows the 12 K spectrum of complex I poised at −0.3 V, using NADH and NAD^+ concentrations defined by the Nernst equation. The g_z components of N4 ($g_z = 2.107$), N2 ($g_z = 2.055$), and N3 ($g_z = 2.041$) are clearly visible, though N3 presents as a shoulder to the right of N2. Two clear g_x signals are observed at $g = 1.884$ and 1.865. They have been attributed previously to N4 and N3, respectively (*8*). As discussed previously (*10*), we attribute N4 to one (or both) of the clusters in the TYKY subunit, 4Fe[TY]1 and 4Fe[TY]2 (see Figure 1). Figure 3 compares the observed spectrum with a modeled spectrum comprising N2, N3 and N4. The N2 parameters are from the spectrum shown in the inset, and the N3 parameters were based on those from FP but with minor modifications. $N3_x$ is shifted in complex I relative to FP, consistent with changes in the environment of 4Fe[51] due to interactions between FP and the rest of complex I; 4Fe[51] is bound by a four helix bundle, and located at the interface with the 75 kDa subunit (*5*). The intensities of N2,

Table 1: EPR Parameters for the Individual Spectra of the Components of Complex I, and Their Variation Depending on the Sample Identity and Reduction State[a]

	Protein	Figures	$g_{z\ or\ ||}$	$g_{y\ or\ \perp}$	$g_{x\ or\ \perp}$	L_z	L_y	L_x	R
FMNH•	FP	2	2.002			0.75			0.01
N1a	24 kDa and FP	2	2.004	1.945	1.917	0.9	1.45	1.2	0.01
N1b	CI (-0.4 V)	4	2.024	1.941	1.926	0.5	0.4	0.5	0
	CI (-1V)	5	2.026	1.945		0.7			
N2	CI	3 – 5	2.055	1.926	1.925	0.5	0.6	0.7	0.01
N3	FP	2	2.037	1.945	1.852	1.25	1	1.9	0.01
	CI (-0.3 and -0.4 V)	3, 4	2.041	1.927	1.865	1.5	1.5	1.1	
	CI (-1V)	5	2.045			0.9		1.7	
N4	CI (-0.3 V)	3	2.107	1.930	1.884	1.4	1.5	1.0	0.01
	CI (-0.4 V)	4	2.114		1.882				
	CI (-1 V)	5	2.109		1.880	1.25		1.8	
N5	CI (-0.3 and -0.4 V)	4	2.064	1.928	1.898	0.6	0.5	0.75	0.01
	CI (-1 V)	5	2.070		1.918			0.5	
Nα	CI (-1 V)	5	2.164	1.919	1.912	1.8	1	1.0	0.01

[a] Each spectrum is defined by one to three g values, the corresponding line widths in mT, and R (the relative contributions from the Lorentzian ($R = 1$) and Gaussian ($R = 0$) line shapes). CI, complex I.

N3 and N4 depend differently on temperature (see Figure S3B). N2 is most visible at 12 and 25 K, N4 is observed at 12 K and below, and N3 is most apparent at 7 to 12 K. An additional spectrum, N5, is observed at the lowest temperatures, with $g_x = 1.898$ and $g_z = 2.064$ (see Figure S3B). Previously we attributed N5 to the all-cysteine ligated [4Fe-4S] cluster in the 75 kDa subunit, 4Fe[75]C (*10*) (see Figure 1); N5 is described below and in Figure 4.

Figure 4 shows spectra from complex I reduced by NADH, at approximately −0.4 V. The obvious difference between Figures 3 and 4 is the appearance of a rhombic spectrum, N1b, attributed to the [2Fe-2S] cluster in the 75 kDa subunit, 2Fe[75]. The clusters which produce N1b, N3, N4 and N5 have previously been considered to have the same potential, and to form an "isopotential pool" (*8*). The results presented here show that the N1b cluster actually has a lower potential than those of N3, N4 and N5, and so should not be considered isopotential with them. N1b is most clearly observed at 40 K (see below), but it contributes over a wide temperature range, at 12 K (Figure 4A), and even at 4 K (Figure 4B) (see also Figure S4, Supporting Information). The relatively weak temperature dependence of N1b has been noted previously (*21*). In Figure 4A the 12 K spectrum has been modeled accurately with the same components as in Figure 3, plus a contribution from N1b. The spectra are normalized to the $N2_z$ signal; in Figure 4 a small increase in the relative intensity of N4 is observed, but the relative intensity of N3 is unchanged. The small observed shift in $N4_z$ has been noted previously (*6, 22*) (see below). The 4 K spectrum (Figure 4B) exhibits the N5 spectrum clearly, in addition to the signals from N1b, N2, N3, and N4.

Complex I at −1 V, Reduced Using Eu^{II}-DTPA. Figure 5 shows the 12 K spectrum from complex I poised with Eu^{II}-DTPA to a potential of approximately −1 V. Eu^{II}-DTPA was detected in the sample as a broad spectrum ($g = 1.1-10$, see Figure S6, Supporting Information) confirming that the potential in solution was close to the reduction potential of Eu^{III}-DTPA (−1.14 V) (*15*). The spectrum in Figure 5 has been modeled using the same components as those in Figures 3 and 4, plus an additional spectrum referred to as Nα (see Table 1), which is used to account for the new signals at $g_z = 2.164$ and $g_x = 1.912$. It is important to realize that the modeling presented in Figure 5 is not a unique solution. It combines six different components, some of which are modified slightly to produce a viable fit to the data, and varying interpretations are possible. In Figure 5 we have increased the intensity of the N3 spectrum, and modified its g values and line widths slightly (see Table 1), instead of introducing an additional spectrum to account for the otherwise "missing intensity". In doing so our aim was to produce as concise an interpretation as possible, rather than to account for changes simply by including extra, uncharacterized components. Thus, Figure 6A compares the 12 K spectra from Figures 3, 4 and 5, and indicates the main differences between them (numbered I to IX). These differences are discussed below, then characterized further using modeling of the spectra and determination of the relaxation properties, to try construct an internally consistent interpretation.

1. The Intensity of N1b Increases Significantly As the Potential Is Decreased (IV, V, VI). It is obvious at 12 K (Figure 6A, IV) that the g_z component of N1b increases each time the potential is decreased. Modeling of the spectra in Figures 4 and 5 suggests that N1b causes much of the change in the g_y region also (Figure 6A, V and VI) since it adds significant positive intensity to V, and negative intensity to VI. The fact that the changes at IV, V and VI are all consistent with an increased contribution from N1b strongly supports the idea that N1b is their common cause. At 12 K (Figure 6A) N1b is approximately 7.2 times more intense at −1 than at −0.4 V (relative to N2). However, the effective

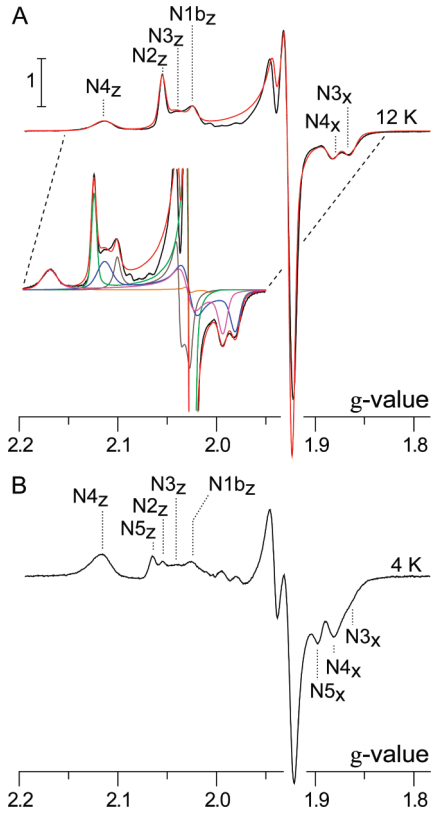

FIGURE 4: EPR spectra of complex I reduced by NADH. Complex I was dialyzed, anaerobically, against a solution (pH 7.8) containing 0.1 mM of purified NADH, and then an additional 2 mM NADH was added immediately before the sample was frozen. (A) The spectrum recorded at 12 K (black) is compared to the simulated spectrum (red). The scale bar refers to the height of the modeled N2$_z$ feature. The inset (not on the same *x*-axis scale) has been expanded 2-fold along the *y*-axis to show how the modeled spectrum comprises N1b (gray), N2 (green), N3 (blue, same intensity as Figure 3), N4 (magenta, 1.1 times the intensity of Figure 3), and N5 (orange). See Table 1 for parameters. (B) The spectrum recorded at 4 K (black) has been expanded by 7.5 times on the *y*-axis, following normalization to temperature according to the Curie Law, to display the signals of N5.

$P_{1/2}$ value for N1b is higher at −1 V than at −0.4 V; the relaxation rate of N1b is increased at the low potential, and this effect contributes to its increased signal intensity. Consequently, Figure 6B compares the spectra of the three samples recorded at 40 K, under conditions in which N1b is not saturated. At 40 K the N1b signal is 3.3 times more intense at −1 V than at −0.4 V, providing a realistic evaluation of the increase in the concentration of the reduced 2Fe[75] cluster. In addition, N1b displays an unusual power saturation profile (see Figure 7A). Similar behavior was observed previously for N5 in the overexpressed NuoG subunit (75 kDa homologue) from *E. coli* complex I (*10*), and may result from dipolar interactions with one or more neighboring paramagnetic centers (*23, 24*). The 2Fe[75] cluster is between two [4Fe-4S] clusters, which may provide these interactions (*5*), and which may explain the increased relaxation rate also.

2. Signals Corresponding to the g_z and g_x of N5 Are Observed at Low Potential at 12 K (III, VIII). Figure 4 shows that N5 is observed clearly only at 4 K in complex I reduced by NADH, consistent with previous consensus (*8*). It is not observed at 12 K, but appears as a broader and less distinct spectrum at 7 and 9 K (see Figure S4). In contrast, Figure 5

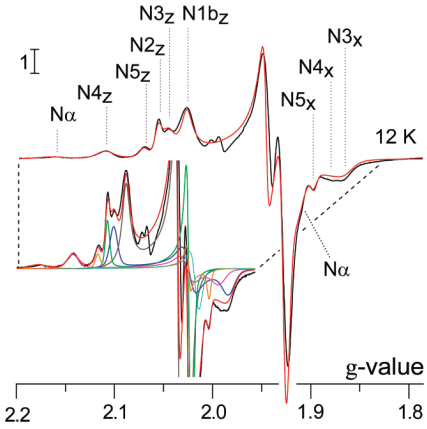

FIGURE 5: EPR spectrum of complex I poised at close to −1 V in the presence of Eu^{II}-DTPA. Complex I was reduced by the addition of 0.65 mM Eu^{II} and 1.3 mM DTPA at pH 7.8. EPR spectra at lower field confirmed the presence of Eu^{II} in the EPR samples (see Figure S6). The spectrum recorded at 12 K (black) is compared to the simulated spectrum (red). The scale bar refers to the height of the modeled N2$_z$ feature. The inset (not on the same *x*-axis scale) has been expanded 2-fold along the *y*-axis to show how the modeled spectrum comprises N1b (gray), N2 (green), N3 (blue), N4 (magenta), an N5-type spectrum (orange) and Nα (cyan). N1b, N3, N4, and the N5-type spectrum are scaled by 7.2, 1.9, 1.2, and 18.2 respectively, relative to Figure 4A. See Table 1 for parameters.

clearly displays features analogous to N5 in the 12 K spectrum of complex I at −1 V. The power saturation profile at the position of N5$_z$ at 9 K (see Figure 7D) shows that $P_{1/2}$ decreases significantly (33-fold) at −1 V relative to at −0.4 V. These intriguing observations indicate that N5 relaxes *more slowly* upon the further reduction of the enzyme, or that there are two clusters with similar *g* values but very different relaxation properties. These two possibilities are discussed below.

3. Further New Signals at $g_z = 2.164$ and $g_x = 1.912$ (I and VII). Two additional features are clearly visible in the −1 V spectrum in Figure 6A, and they may indicate the reduction of a further iron−sulfur cluster. In Figure 5 they have been reproduced simply by including the contribution from a rhombic spectrum with $g_z = 2.164$ and $g_x = 1.912$ (see Table 1) [alternatively, these two signals may also cross match to the two N5-type signals described above, rather than to each other]. However, a g_z value of 2.164 is unusually high for a [4Fe-4S] cluster, indicating that a more likely explanation is that it represents the coupling of two adjacent reduced clusters (see below).

4. Modification of the N3 and N4 Spectra at Low Potential (II, IX). Figure 6A shows clearly that N4$_z$ is not well conserved between the three samples, and that the "envelope" created by N3$_x$ and N4$_x$ has changed in shape, from "W" at higher potential to "U" at low potential. Corresponding shifts in N4$_z$ noted previously were used to suggest that it comprises two overlapping signals, or that spin−spin interactions or a conformational change are present (*6, 22*). Interestingly, in these analyses N4 was found to provide spin concentrations approximately equal to that of the flavin, irrespective of whether it was considered as one or two clusters. Our model also includes a small shift and increase in the width of N4$_x$ (see Table 1) and a moderate (20%) increase in the relative intensity of N4 upon reduction to −1 V. Notably, the relaxation properties of the clearly defined N4$_z$ feature are unchanged (see Figure 7C).

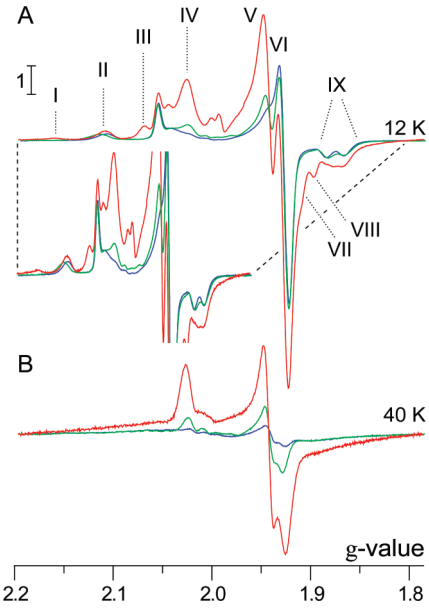

FIGURE 6: Comparison of the low potential spectra of complex I with the spectra at −0.3 and −0.4 V. (A) The spectra were recorded at 12 K (taken from Figures 3, 4 and 5) and normalized using the intensity of the modeled $N2_z$ feature (indicated by the scale bar): −0.3 V (blue), −0.4 V (green), −1 V (red). The inset (not on the same *x*-axis scale) has been expanded 2-fold along the *y*-axis. Differences between them are numbered as follows. I, a new signal at $g = 2.16$ in the −1 V sample. II, $N4_z$ is not strictly conserved. III, a signal corresponding to $N5_z$ is observed at −1 V. IV, $N1b_z$ is strongly enhanced at −1 V. V and VI, the spectrum from the overlapping g_y signals varies significantly; VII, a shoulder is observed at $g = 1.91$ at −1 V. VIII, a signal corresponding to $N5_x$ is present at −1 V; IX, the envelope formed by $N4_x$ and $N3_x$ changes shape from "W" at high potential to "U" at low potential. In addition, two small signals are apparent at −1 V at $g = 2.001$ and 1.993. They have been observed previously in different sets of samples: their origin is unknown, but they do not correlate to the sample potential. (B) The spectra were recorded at 40 K. They are reported on the same scale as A, following temperature normalization according to the Curie Law.

On first inspection the W to U transition at g_x suggests an additional contribution to the spectrum (at $g \sim 1.873$) to fill the gap between $N3_x$ and $N4_x$. A more concise interpretation, which also accurately reproduces the observed spectrum, is that (in addition to the changes in N4 noted above) N3 increases in intensity and $N3_x$ shifts and broadens slightly (see Table 1). Additional intensity and a slight sharpening of $N3_z$ improve the quality of the fit at $g \sim 2.04$ also. Measurements of the dependence of the signal intensity at the position of $N3_x$ on microwave power gave the same $P_{1/2}$ values for the samples at −0.4 and −1 V ($P_{1/2} = 3.5$ mW). It is difficult to characterize the power saturation behavior of $N3_z$ because it is not clearly resolved, but the $P_{1/2}$ value measured between $N3_x$ and $N4_x$ ($g = 1.873$) did not change either ($P_{1/2} = 2$ mW). On the other hand, the increased intensity of N3 is questionable; there is a general consensus that N3 is already fully reduced in NADH-reduced complex I, so the possibility of an additional contribution from an unknown spectrum cannot be excluded.

DISCUSSION

Comparison of the N1b, N2, N3, N4 and N5 Spectra with Those Described Previously. Extensive research efforts over many years have defined clearly five EPR spectra from

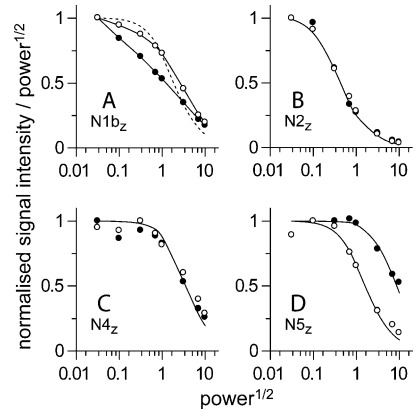

FIGURE 7: Comparison of power saturation profiles at characteristic *g* values in complex I reduced by NADH and by Eu^{II}-DTPA. The intensities were recorded at the characteristic *g* values reported in Table 1. (●) NADH reduced sample; (○) Eu^{II}-DTPA reduced sample. The spectra were recorded at 9 K, and each profile was normalized to its highest value, I_0. The data were fit using the relationship $I/(I_0P^{1/2}) = (1 + P/P_{1/2})^{-b/2}$ where *I* is the intensity, $I \rightarrow I_0$ as $P \rightarrow 0$, *P* is the microwave power, $P_{1/2}$ is the power at half-saturation, and *b* is the homogeneity factor, ideally $b = 1$ at the inhomogeneous limit (*23, 24*). The dotted line for $N1b_z$ denotes the case for which $b = 1$.

reduced complex I from mitochondria, and these spectra are the basis for the modeling described here. Close agreement is noted between the *g* values found here and the values reported earlier (*8*) (see Table S2, Supporting Information).

A significant (more than 3-fold) increase in the relative intensity of N1b was found here between the −0.4 and −1 V samples. N1b is not observed at −0.3 V and is significantly increased below −0.4 V, so it does not form an "isopotential pool" with N3, N4 and N5 (as previously discussed (*8*)) but has a lower potential than they do. We note that previous measurements of the reduction potential of N1b were recorded over a more limited range of potential than accessed here, that they were complicated by confusion about the similarity of the N1a and N1b spectra (see below), and that they did not consider the possibility that N1b becomes reduced over an extended range of potential. A broad titration curve for N1b has been elucidated recently for *E. coli* complex I, and attributed to electrostatic interactions between neighboring clusters (*25*). Our observation clearly contradicts Ohnishi's statement that N1b, N2, N3 and N4 are present in a relative stoichiometry of 1:1:1:1 in complex I reduced by NADH (*8*) also. However, a range of values have been reported in the literature (reviewed in refs *7* and *21*), and, based on a number of different methods of analysis, Albracht and co-workers long contended that reduced N1b is present at only 0.5 times the concentration of reduced N2 in complex I reduced by NADH (*21*).

During this work we attempted to evaluate the relative intensities of the different spectra within a single sample but found it deceptively difficult. Not only is it difficult to construct an accurate deconvolution, particularly in the g_y region and where g_z and g_x signals overlap, but it is not possible to make all the spectra unsaturated within one single spectrum, so that corrections and cross-references have to be applied. We note that, between the −0.4 and −1 V samples, the estimated relative intensities of N3 and N4 also increase by 1.9- and 1.2-fold, respectively. As all our intensities are reported relative to N2, we cannot discount

the possibility that the N2 intensity has actually decreased, and it is tempting, though unwarranted at this stage, to speculate about changes in conformation, cluster ligation, or coupling to semiquinone or the clusters in the TYKY subunit. Further investigation of these intriguing ideas is outside the scope of the current work.

N1a Is Not Observed in Complex I Reduced to −1 V. EPR spectrum N1a, from the 2Fe[24] cluster, is defined clearly by the overexpressed 24 kDa subunit and by subcomplex FP reduced by dithionite (see Figure 2), but N1a is not observed in FP reduced by NADH. It is likely that the cluster's reduction potential is below that of NADH, but constraints from the two-electron reaction of NADH may also be limiting. When FP (containing only three redox centers) is reduced by two electrons, the most stable state thermodynamically is that with one electron on the flavin and one on cluster 4Fe[51] (N3). Thus, NADH promotes the formation of the semiquinone in FP, and, indeed, Figure 2D shows a corresponding increase in its signal. The fully reduced, four-electron state is thermodynamically and/or kinetically inaccessible to NADH, and its formation may be impeded by electron density at the flavin active site also. In contrast, complex I contains nine redox centers; they provide many different possibilities for distributing the electrons (relaxing the constraint which is observed in FP) and so the flavin semiquinone is much less prominent.

It is difficult to explain why N1a is not observed in complex I at any potential, even at −1 V. Initially, the N1a and N1b spectra were considered essentially indistinguishable, and this has led to confusion because values for the reduction potential of N1a have been reported (in addition, the reduction potential for N1b was found to be higher than its true value). There is now sufficient evidence to conclude that the spectrum observed in mitochondrial complex I is from N1b alone (*10, 13, 26*), so that the reduction potential of N1a is not in fact known, and N1b exhibits an extended potential dependence (*25*). In *E. coli* complex I N1a has a higher potential (from comparison of the cluster potentials in the overexpressed subunits (*16*)), and it is clearly visible in spectra recorded at around 40 K (*10, 12, 27*). This fact, and the spectra of FP, argue against 2Fe[24] being reduced but N1a not being observed, for example, because of its interactions with the reduced flavin. It is possible that 2Fe[24] remains oxidized for either thermodynamic or kinetic reasons.

Thermodynamically, increasing the number of electrons in complex I builds up electrostatic interactions between the reduced clusters, and undoubtedly makes the addition of further electrons less favorable. However, it is unlikely that such interactions are sufficient to shift the apparent potential of N1a to below −1 V, even if it is the last cluster in complex I to become reduced (note that this effect would not necessarily affect 2Fe[24] under steady state conditions, as then the enzyme is not reduced to this extreme level). Kinetically, it is unlikely that the direct reduction of 2Fe[24] (unmediated electron transfer from a species in solution) is possible in complex I due to "insulation" from the supernumerary subunits, and it is assumed (but not proven) that the relative positions of the flavin and 2Fe[24] are conserved between bovine and *T. thermophilus* complex I, so that the cluster is within easy tunneling range (*5*). However, kinetic limitations may result from the potential of the flavin being above that of 2Fe[24], making cluster reduction by the flavin unfavorable. Furthermore, if the rate at which Eu^{II}-DTPA reacts with complex I is determined by the availability of an oxidized state of the flavin, then it will decrease significantly as the potential is decreased. For example, the rate of reaction at −0.8 V will be approximately 10^7 times slower than at −0.4 V, so that a reaction half-time of 0.35 ms at −0.4 V (assuming a turnover number of 2000 s^{-1} (*28*)) becomes approximately 1 h at −0.8 V. Therefore, it is likely that full reduction of complex I is simply not achieved during the time scale on which sample preparation is possible. Similar reasoning may explain previous observations that dithionite reduces N2, N3 and N4 in complex I, but not N1b, despite its potential clearly being low enough to do so (*29*).

The Unusual Behavior of N5. EPR spectrum N5 is observed in the mitochondrial complexes I from bovine heart (*8*) and *Yarrowia lipolytica* (*30*), but it has not been observed in complex I from *E. coli*. In mitochondrial complex I it is the fastest relaxing spectrum, so is observed at low temperature and high power. The *g* values of N5 (g_{zyx} = 2.06−7, 1.93, 1.90−2) correlate closely to those of a spectrum from the overexpressed 75 kDa subunits from *Paracoccus denitrificans* (*31, 32*) and *E. coli* (*33*). Consequently, N5 was assigned to the 75 kDa subunit (*10*). However, two aspects of this assignment may be questioned. First, the N5 spectrum from mitochondrial complex I is matched to a spectrum from the overexpressed subunits of two bacterial enzymes, though the bacterial enzymes do not themselves display N5. The assumption is that all complexes I contain the same complement of clusters, even though different cluster subsets are reduced upon reaction with NADH. Second, the relaxation rate of the N5-type spectrum is different in the two cases (it is observed at 4 K in mitochondrial complex I, 12 K in the overexpressed subunits), perhaps because it responds to the presence or absence of adjacent subunits and clusters.

Figure 4B shows that N5 is observed at 4 K at −0.4 V (and not above 9 K, see Figure S4), but Figure 5 shows that signals with the same *g* values are observed at 12 K at −1 V (as well as at 4 K, see Figure S5, Supporting Information). The difference is reflected in the power saturation data (see Figure 7D). It is difficult to imagine how a cluster can relax more slowly at lower potential, since the reduction of any nearby cluster would lead to the formation (not the destruction) of a paramagnet. Two possible explanations are a significant conformational change which changes the properties of the cluster, or the existence of two clusters giving rise to N5-type spectra with similar *g* values but different relaxation properties. Both explanations have advantages and disadvantages. There is no apparent reason for a significant conformational change at N5 (assigned to 4Fe[75]C (*10*)), the only reasonable possibility being a change resulting from the EPR-silent reduction of 4Fe[75]H (see below). The existence of two N5-type clusters would modify the established assignments of EPR spectra to structurally defined clusters. The "high temperature" N5 spectrum is observed in mitochondrial complex I at −1 V and in the overexpressed subunits, suggesting that this spectrum arises from 4Fe[75]C (it is not affected by mutation of the histidine residue) (*32, 33*). The "low-temperature" N5 spectrum observed only in mitochondrial complex I does not arise from 4Fe[75]H, since it is not affected by mutation of the histidine residue either (*30*), so it can only be assigned to TYKY. The two possibilities are illustrated in Figure 8.

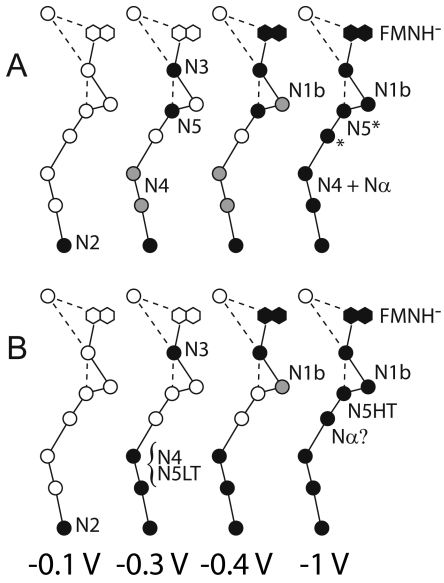

FIGURE 8: Two possible patterns of cofactor reduction in bovine complex I. At −0.1 V only spectrum N2 is observed. At −0.3 V the N3, N4 and N5 spectra are visible also. In (A) N4 is from TYKY and N5 is from the 75 kDa subunit, in (B) both N4 and the low temperature N5 (N5LT) spectrum are from TYKY. At −0.4 V N1b is partially reduced. At −1 V N1b is fully reduced, and it is influenced by the reduction of a nearby cluster (N5* or N5HT). In (A) the characteristics of N5 are altered (N5*), perhaps because 4Fe[75]H is reduced (*), and Nα arises from the interaction of the two clusters in TYKY. In (B) 4Fe[75]C produces the high-temperature N5 (N5HT) spectrum, and the only possibility for Nα is to assign it to 4Fe[75]H.

Evidence for Intercluster Interactions. There are eight FeS clusters in complex I, seven of which are in a continuous chain, so coupling effects between reduced clusters are to be anticipated as the cluster ensemble becomes more reduced. In complex I, spin−spin interactions between flavin semiquinone and N3 (*14*), and between ubisemiquinone and N2 (*34, 35*), have been well documented. Similar interactions between two reduced clusters, however, have been less widely recognized, although Albracht and co-workers suggested that the effects on the $N2_z$ signal (ascribed otherwise to its coupling to ubisemiquinone) actually originate from spin−spin interactions between 4Fe[TY]1 and 4Fe[TY]2 (*36*). It is likely that the additional features observed at −1 V, described above as Nα, result from two interacting reduced clusters. The apparent g_z signal at 2.16 is unusually high for a reduced [4Fe-4S] cluster, and reminiscent of the $g_{app} = 2.18$ feature in the spectra of fully reduced 8Fe ferredoxins (*37*), and in fully reduced FeS-containing enzymes such as succinate dehydrogenase ($g_{app} = 2.27$) (*38*). The complexity of the underlying complex I spectrum makes it difficult to distinguish additional features of the coupled spectrum at present, though it may contribute to the increased intensity observed at the N1b or N3 g_z values, and possibly to the small shifts observed in N3 and N4. Future investigation using different microwave frequencies will help to characterize Nα further.

An additional interaction between the clusters in complex I is suggested by the increased apparent $P_{1/2}$ value for N1b at low potential (Figure 7A), indicating that a nearby cluster has become reduced. Three clusters are within 20 Å of N1b: 4Fe[51] (N3, which is already reduced), 4Fe[75]C, and 4Fe[75]H (*5*). Interpretation of the increased apparent $P_{1/2}$ value of N1b depends on the identity of N5 (see above). If 4Fe[75]C provides the high-temperature N5 signal, then reduction of this cluster probably affects the relaxation rate of N1b. If N5 is only from 4Fe[75]C, then the change which affects N5 may also affect N1b. The possibility that the "EPR-silent" reduction of 4Fe[75]H is responsible for the increased relaxation rate of N1b is reminiscent of the enhanced spin relaxation properties of [2Fe-2S] cluster S1 in succinate dehydrogenase upon the reduction of [4Fe-4S] cluster S2 (*38*). It is possible that the 4Fe[75]H cluster has not been observed by EPR because it exists in a higher spin state, as does the histidine-ligated [4Fe-4S] cluster in nitrate reductase A (*39*).

Implications for Electron Transfer in Complex I. Figure 8 illustrates two possible explanations for the results described above, and summarizes the electron distribution in complex I at each potential. The "reduction pattern" results from the potentials of the clusters, and from electrostatic interactions between them. The "operating potential" of complex I in the mitochondrion is represented best by the sample at −0.3 V, because NADH oxidation is fast with respect to quinone reduction, and because the mitochondrial NAD^+/ NADH pool is 90% oxidized. At −0.3 V there are probably four electrons in the cofactor chain. Consequently, calculations of the rate of electron transfer from flavin to quinone need to take into account the occupancy of the chain, as well as the potentials of the individual clusters and the rates of electron transfer between them. This "occupancy effect" means that the rate at which two electrons leave the flavin and arrive at the quinone site (not necessarily the same two electrons) is probably considerably higher than calculations which do not account for the occupancy effect suggest. Nevertheless, by using potentials of −0.25 V for every cluster except N1a (−0.38 V) and N2 (−0.1 V) Moser and co-workers calculated an electron transit time of approximately 100 μs (for one electron moving from flavin to N2) (*40*), similar to the rate of NADH:hexaammineruthenium-(III) oxidoreduction at the flavin site (∼5000 electrons s^{-1} (*28*)). Although uncertainty in the cluster potentials may affect the calculated values, the comparison indicates that electron transfer along the cluster chain is probably much faster than the rate of catalysis, making complex I robust toward changes in any one of the individual cluster potentials. Interestingly, the two models in Figure 8 suggest quite different arrangements of the electrons in the "loaded" enzyme (in Figure 8A they are spaced evenly across the chain, but in Figure 8B three of the four are queued behind the quinone binding site). It is possible that the prearrangement affects the sequential delivery of two electrons to bound quinone.

SUPPORTING INFORMATION AVAILABLE

Comparison of the principal g values of modeled spectra with their published equivalents; spectra recorded over a range of temperature for each sample analyzed; wide-field spectrum of Eu^{II} sample. This material is available free of charge via the Internet at http://pubs.acs.org.

REFERENCES

1. Sazanov, L. A. (2007) Respiratory complex I: mechanistic and structural insights provided by the crystal structure of the hydrophilic domain. *Biochemistry 46*, 2275–2288.

2. Brandt, U. (2006) Energy converting NADH:quinone oxidoreductase (complex I). *Annu. Rev. Biochem. 75*, 69–92.
3. Hirst, J. (2005) Energy transduction by respiratory complex I - an evaluation of current knowledge. *Biochem. Soc. Trans. 33*, 525–529.
4. Carroll, J., Fearnley, I. M., Skehel, J. M., Shannon, R. J., Hirst, J., and Walker, J. E. (2006) Bovine complex I is a complex of 45 different subunits. *J. Biol. Chem. 281*, 32724–32727.
5. Sazanov, L. A., and Hinchliffe, P. (2006) Structure of the hydrophilic domain of respiratory complex I from *Thermus thermophilus*. *Science 311*, 1430–1436.
6. Ohnishi, T. (1979) Mitochondrial iron-sulfur flavodehydrogenases, in *Membrane Proteins in Energy Transduction* (Capaldi, R., Ed.) pp 1−87, Marcel Dekker, New York.
7. Beinert, H., and Albracht, S. P. J. (1982) New insights, ideas and unanswered questions concerning iron-sulfur clusters in mitochondria. *Biochim. Biophys. Acta 683*, 245–277.
8. Ohnishi, T. (1998) Iron-sulfur clusters/semiquinones in complex I. *Biochim. Biophys. Acta 1364*, 186–206.
9. Hirst, J., Carroll, J., Fearnley, I. M., Shannon, R. J., and Walker, J. E. (2003) The nuclear encoded subunits of complex I from bovine heart mitochondria. *Biochim. Biophys. Acta 1604*, 135–150.
10. Yakovlev, G., Reda, T., and Hirst, J. (2007) Reevaluating the relationship between EPR spectra and enzyme structure for the iron-sulfur clusters in NADH:quinone oxidoreductase. *Proc. Natl. Acad. Sci. U.S.A. 104*, 12720–12725.
11. Esterházy, D., King, M. S., Yakovlev, G., and Hirst, J. (2008) Production of reactive oxygen species by complex I (NADH: ubiquinone oxidoreductase) from *Escherichia coli*, and comparison to the enzyme from mitochondria. *Biochemistry 47*, 3964–3971.
12. Uhlmann, M., and Friedrich, T. (2005) EPR signals assigned to Fe/S cluster N1c of the *Escherichia coli* NADH:ubiquinone oxidoreductase (complex I) derive from cluster N1a. *Biochemistry 44*, 1653–1658.
13. Hearshen, D. O., Dunham, W. R., Albracht, S. P. J., Ohnishi, T., and Beinert, H. (1981) EPR spectral simulation on cluster N-1b in NADH-ubiquinone oxidoreductase of bovine heart mitochondria. *FEBS Lett. 133*, 287–290.
14. Sled, V. D., Rudnitzky, N. I., Hatefi, Y., and Ohnishi, T. (1994) Thermodynamic analysis of flavin in mitochondrial NADH: ubiquinone oxidoreductase (complex I). *Biochemistry 33*, 10069–10075.
15. Vincent, K. A., Tilley, G. J., Quammie, N. C., Streeter, I., Burgess, B. K., Cheesman, M. R., and Armstrong, F. A. (2003) Instantaneous, stoichiometric generation of powerfully reducing states of protein active sites using Eu(II) and polyaminocarboxylate ligands. *Chem. Commun. 20*, 2590–2591.
16. Zu, Y., di Bernardo, S., Yagi, T., and Hirst, J. (2002) Redox properties of the [2Fe-2S] center in the 24 kDa (NQO2) subunit of NADH:ubiquinone oxidoreductase (complex I). *Biochemistry 41*, 10056–10069.
17. Barker, C. D., Reda, T., and Hirst, J. (2007) The flavoprotein subcomplex of complex I (NADH:ubiquinone oxidoreductase) from bovine heart mitochondria: insights into the mechanisms of NADH oxidation and NAD^+ reduction from protein film voltammetry. *Biochemistry 46*, 3454–3464.
18. Sharpley, M. S., Shannon, R. J., Draghi, F., and Hirst, J. (2006) Interactions between phospholipids and NADH:ubiquinone oxidoreductase (complex I) from bovine mitochondria. *Biochemistry 45*, 241–248.
19. Orr, G. A., and Blanchard, J. S. (1984) High-performance ion-exchange separation of oxidized and reduced nicotinamide adenine dinucleotides. *Anal. Biochem. 142*, 232–234.
20. Ragan, C. I., Galante, Y. M., Hatefi, Y., and Ohnishi, T. (1982) Resolution of mitochondrial NADH dehydrogenase and isolation of two iron-sulfur proteins. *Biochemistry 21*, 590–594.
21. van Belzen, R., de Jong, A. M. P., and Albracht, S. P. J. (1992) On the stoichiometry of the iron-sulfur clusters in mitochondrial NADH:ubiquinone oxidoreductase. *Eur. J. Biochem. 209*, 1019–1022.
22. Orme-Johnson, N. R., Hansen, R. E., and Beinert, H. (1974) Electron paramagnetic resonance-detectable electron acceptors in beef heart mitochondria. *J. Biol. Chem. 249*, 1922–1927.
23. Hirsh, D. J., Beck, W. F., Innes, J. B., and Brudvig, G. W. (1992) Using saturation-recovery EPR to measure distances in proteins: applications to photosystem II. *Biochemistry 31*, 532–541.
24. Galli, C., Innes, J. B., Hirsh, D. J., and Brudvig, G. W. (1996) Effects of dipole-dipole interactions on microwave progressive power saturation of radicals in proteins. *J. Magn. Reson. B 110*, 284–287.
25. Euro, L., Bloch, D. A., Wikström, M., Verkhovsky, M. I., and Verkhovskaya, M. (2008) Electrostatic interactions between FeS clusters in NADH:ubiquinone oxidoreductase (complex I) from *Escherichia coli*. *Biochemistry 47*, 3185–3193.
26. Zickermann, V., Zwicker, K., Tocilescu, M. A., Kerscher, S., and Brandt, U. (2007) Characterization of a subcomplex of mitochondrial NADH:ubiquinone oxidoreductase (complex I) lacking the flavoprotein part of the N-module. *Biochim. Biophys. Acta 1767*, 393–400.
27. Leif, H., Sled, V. D., Ohnishi, T., Weiss, H., and Friedrich, T. (1995) Isolation and characterization of the proton-translocating NADH:ubiquinone oxidoreductase from *Escherichia coli*. *Eur. J. Biochem. 230*, 538–548.
28. Yakovlev, G., and Hirst, J. (2007) Transhydrogenation reactions catalyzed by mitochondrial NADH-ubiquinone oxidoreductase (complex I). *Biochemistry 46*, 14250–14258.
29. Kowal, A. T., Morningstar, J. E., Johnson, M. K., Ramsay, R. R., and Singer, T. P. (1986) Spectroscopic characterization of the number and type of iron-sulfur clusters in NADH:ubiquinone oxidoreductase. *J. Biol. Chem. 261*, 9239–9245.
30. Waletko, A., Zwicker, K., Abdrakhmanova, A., Zickermann, V., Brandt, U., and Kerscher, S. (2005) Histidine 129 in the 75-kDa subunit of mitochondrial complex I from *Yarrowia lipolytica* is not a ligand for $[Fe_4S_4]$ cluster N5 but is required for catalytic activity. *J. Biol. Chem. 280*, 5622–5625.
31. Yano, T., Yagi, T., Sled, V. D., and Ohnishi, T. (1995) Expression and characterization of the 66-Kilodalton (NQO3) iron-sulfur subunit of the proton-translocating NADH-quinone oxidoreductase of *Paracoccus denitrificans*. *J. Biol. Chem. 270*, 18264–18270.
32. Yano, T., Sklar, J., Nakamaru-Ogiso, E., Takahashi, Y., Yagi, T., and Ohnishi, T. (2003) Characterization of cluster N5 as a fast-relaxing [4Fe-4S] cluster in the Nqo3 subunit of the proton-translocating NADH-ubiquinone oxidoreductase from *Paracoccus denitrificans*. *J. Biol. Chem. 278*, 15514–15522.
33. Nakamaru-Ogiso, E., Yano, T., Yagi, T., and Ohnishi, T. (2005) Characterization of the iron-sulfur cluster N7 (N1c) in the subunit NuoG of the proton-translocating NADH-quinone oxidoreductase from *Escherichia coli*. *J. Biol. Chem. 280*, 301–307.
34. Vinogradov, A. D., Sled, V. D., Burbaev, D. S., Grivennikova, V. G., Moroz, I. A., and Ohnishi, T. (1995) Energy-dependent complex I-associated ubisemiquinones in submitochondrial particles. *FEBS Lett. 370*, 83–87.
35. Yano, T., Dunham, W. R., and Ohnishi, T. (2005) Characterization of the $\Delta\mu_{H+}$-sensitive ubisemiquinone species (SQ_{Nf}) and the interaction with cluster N2: new insight into the energy-coupled electron transfer in complex I. *Biochemistry 44*, 1744–1754.
36. van Belzen, R., Kotlyar, A. B., Moon, N., Dunham, W. R., and Albracht, S. P. J. (1997) The iron-sulfur clusters 2 and ubisemiquinone radicals of NADH:ubiquinone oxidoreductase are involved in energy coupling in submitochondrial particles. *Biochemistry 36*, 886–893.
37. Mathews, R., Charlton, S., Sands, R. H., and Palmer, G. (1974) On the nature of the spin coupling between the iron-sulfur clusters in the eight-iron ferredoxins. *J. Biol. Chem. 249*, 4326–4328.
38. Maguire, J. J., Johnson, M. K., Morningstar, J. E., Ackrell, B. A. C., and Kearney, E. B. (1985) Electron paramagnetic resonance studies of mammalian succinate dehydrogenase; detection of the tetranuclear cluster S2. *J. Biol. Chem. 260*, 10909–10912.
39. Rothery, R. A., Bertero, M. G., Cammack, R., Palak, M., Blasco, F., Strynadka, N. C. J., and Weiner, J. H. (2004) The catalytic subunit of *Escherichia coli* nitrate reductase A contains a novel [4Fe-4S] cluster with a high-spin ground state. *Biochemistry 43*, 5324–5333.
40. Moser, C. C., Farid, T. A., Chobot, S. E., and Dutton, P. L. (2006) Electron tunneling chains of mitochondria. *Biochim. Biophys. Acta 1757*, 1096–1109.

BI800437G